

Stainless Steels as Sustainable Solution for Concrete Reinforcement - from Laboratory to Practice

ELSENER Bernhard^{1,2,a*}, Fantauzzi Marzia^{1,b} and ROSSI Antonella^{1,c}

¹Departement of Chemical and Geological Sciences, University of Cagliari, 09140 Cagliari, Italy

²ETH Zurich, Institute of Building Materials, Stefano Franscini Platz 5, 8093 Zurich, Switzerland

^aelsener@ethz.ch, ^bfantauzzi@unica.it, ^crossi@unica.it

Keywords: Stainless Steels, reinforcement, concrete, passivation, XPS surface analysis, pitting, critical chloride content

Abstract. Stainless steel reinforcing bars show excellent corrosion resistance in concrete exposed to harsh environments. In this combined electrochemical and surface analytical work, an explanation for this behavior is proposed. XPS surface analytical results (thickness, composition of the passive film and of the interface beneath the film) obtained on black steel, FeCr alloys, and a series of stainless steels after exposure to alkaline solutions simulating concrete are reported. Pitting potentials were determined in the same solutions with electrochemical experiments. It is shown that the pitting potentials of the steels can be related to the Cr(III)oxy-hydroxide and Mo(VI) content in the passive film. It is proposed to calculate a Cr and Mo oxide equivalent similar to the well-known pitting resistance equivalent number (PREN). A correlation between the critical chloride content in concrete (reported in literature for CEM II A/LL and CEM I) and the pitting potential for carbon steel, Fe12%Cr alloy, DIN 1.4301 and DIN 1.4571 stainless steels is proposed to link results of solution analysis and performance in concrete.

Introduction

Corrosion of the reinforcement due to chloride ions penetrating into concrete is the main cause of early damage, loss of serviceability and very high repair costs of reinforced concrete structures [1, 2]. Austenitic and duplex stainless steels require up to 10 times higher chloride content to initiate corrosion in concrete and thus can prevent reinforcement corrosion in marine or road environments with very high chloride concentrations [3, 4]. A well-documented example of the long-term performance of stainless steel reinforcement is the pier Progresso in the Gulf of Mexico, entirely constructed using 18Cr8Ni stainless steel in the forties of last century. In this example no corrosion has been observed even after nearly 70 years [5]. More recent prestigious bridges such as the Stonecutters' bridge in Hong Kong have used stainless steels in the outermost reinforcement layers [6].

A critical issue when using stainless steels as reinforcement for concrete structures is the 6 to 10 times higher material cost that leads to higher total construction costs [7]. The most cost optimal solution is the employment of stainless steel reinforcement in the most exposed zones/parts of the structure. As the benefit on the long-term, the lower total life-cycle costs, not always convinces the owner, research and industry developed "low-cost" stainless steels, but their resistance against chloride induced localized corrosion and especially the long-term behaviour in concrete is not yet established.

A recent paper of the authors in the Encyclopaedia of Interfacial Chemistry [8 and literature cited therein] summarizes the knowledge in the field of passivation of steels and stainless steels in alkaline media, combining results from electrochemical and surface analytical studies. Based on our work [9 - 11] and on literature data, this paper addresses two important issues: first, the pitting potentials from solution experiments is rationalized with the chemical state and composition of the surface film. Second, a correlation between the pitting potentials obtained in short-term solution tests with the critical chloride content for corrosion initiation in concrete is proposed.

Experimental

Materials. The composition of the materials investigated in this work is given in table 1. The surface of the alloys was first ground with emery paper in water and then mirror-like polished using diamond pastes up to 1 μm (Struers, Bellerup DK) using analytical grade ethanol. Samples were washed with ethanol and dried in an argon stream.

Table 1: Composition (wt.%) of the steels and pitting resistant equivalent number (PREN) calculated as $\%Cr + 3.3*\%Mo$

Alloy	Cr	Ni	Mn	Mo	Others	AISI equivalent	PREN
1.0037	-	-	-	-		1015	0
Fe15Cr	15	-	-	-	-		15
1.4301	18.1	8.7	-	< 0.1	S 0.003	304	18
1.4462	21.8	5.6	-	2.9	S 0.005	318 LN	32
1.4456	17.9	0.2	18.4	1.9	S 0.004		24

Solutions. The mechanically polished samples were exposed to two different solutions simulating the concrete pore environment:

1. 0.1 M NaOH, pH 13
2. Synthetic pore solution, 0.25 M KOH + 0.02 M NaOH + 0.01 M Na_2SO_4 + 0.0001 M $\text{Ca}(\text{OH})_2$, pH 13.2. The synthetic pore solution was based on results of pore solution expression of mortar with CEM I w/c ratio 0.5 [2].

Chloride ions in a range from 0.1 to 5 M NaCl were added to these alkaline solutions. All solutions were stored in a vessel of 1 dm^3 and de-aerated for one day with argon gas. Argon bubbling was prolonged during the measurements.

Electrochemical tests. An Autolab potentiostat/galvanostat (ECO Chemie NL) was used for the measurements in a three-electrode electrochemical cell. Polarization curves were recorded with a scan rate 0.2 mV/s, the potentiostatic tests were performed at -0.1 V SCE. All potentials are referred to the saturated calomel electrode (SCE).

At least two independent measurements were carried out in this study for each material/solution combination here investigated. More details are reported in [10].

XPS surface analysis. At the end of the electrochemical tests (OCP and potentiostatic test) the samples were washed with distilled water, dried in a stream of Argon and transferred in less than one minute to the fast entry lock of the spectrometer with a vacuum of ca. 10^{-5} Pa.

XPS analysis was performed with a Theta Probe ARXPS spectrometer (Thermo Fischer Scientific) using the $\text{AlK}\alpha$ source at 70 W. The analyser was operated in the fixed analyser transmission mode. Three points with a spot size of 300 μm were analysed on each sample. The residual pressure in the UHV chamber was always lower than $5*10^{-7}$ Pa.

Data processing is described in detail elsewhere [10]. Thickness and composition of the passive films grown on the three alloys and the composition of the metal interface beneath the film have been calculated using a three-layer model [8]. The calculations were based on the integrated XPS intensities of the different components that were corrected for Scofield's photo-ionization cross-sections, the instrument transmission function and the inelastic mean free path (IMFP) [8].

Results

Passivation. The open circuit potential (OCP) of all the alloys shortly after immersion into the alkaline solutions was around -500 ± 20 mV SCE and increased asymptotically upon time. The OCP values after 1 d of immersion were found at $-320 \text{ mV} \pm 30 \text{ mV}$ SCE for all alloys in both alkaline solutions (Fig. 1), indicating the spontaneous formation of a protective passive film [8]. In

other alkaline and chloride containing solutions OCP values in the same range were reported [9, 10].

Potentiostatic passivation at the imposed potential of -0.1 V SCE in the alkaline 0.1 M NaOH and in the pore solution showed a continuous decrease of the current density for all the alloys following a power law with approximately a slope of -0.8, close to the theoretical value of -1. The current densities are highest for the Fe15Cr model alloy, about a factor 2 – 3 lower for the stainless steel 1.4301 and for the duplex 1.4462 one. After one day the passive current density is in the order of 10 – 20 nA/cm² (Fig. 2).

All the samples were analysed by XPS at the end of the electrochemical test.

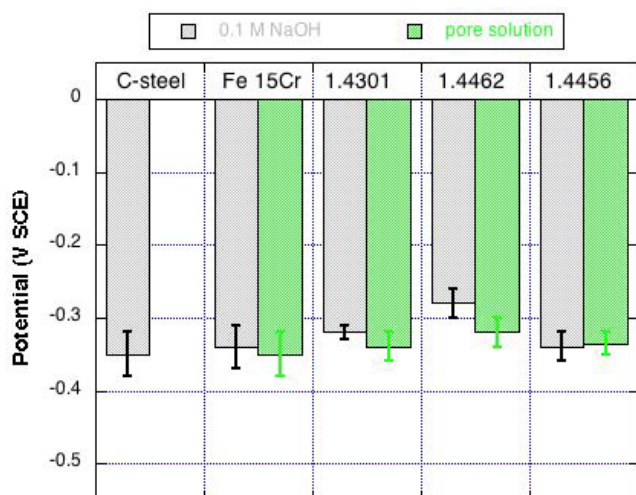


Figure 1: Open circuit potential after 1 day immersion in 0.1 M NaOH and pore solution

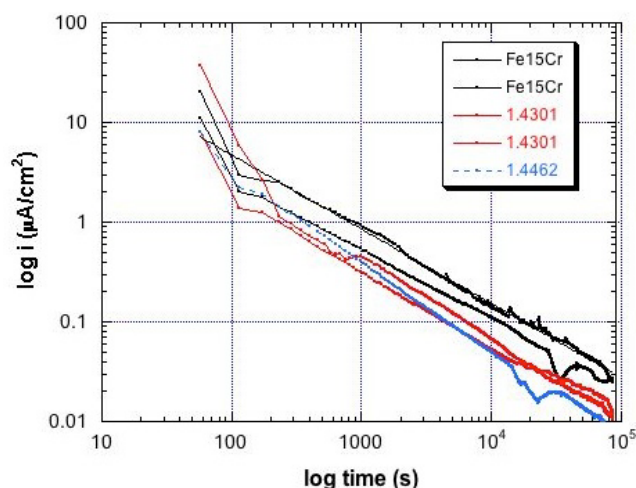


Figure 2: Potentiostatic passivation in 0.1 M NaOH at the potential of -0.1 V SCE

X-ray photoelectron spectra. The surface of the stainless steel samples was analysed after exposure at the OCP and after potentiostatic polarization at -0.1 V SCE in 0.1 M NaOH and in the synthetic pore solution. The survey spectra (not shown) only exhibited x-ray photoelectron and Auger induced signals from the alloy constituents and carbon and oxygen that are due to the sample exposure to the solution and to the atmosphere. No traces of ions from the solutions (Na^+ , K^+ , Ca^{2+} , Cl^- and SO_4^{2-}) were revealed.

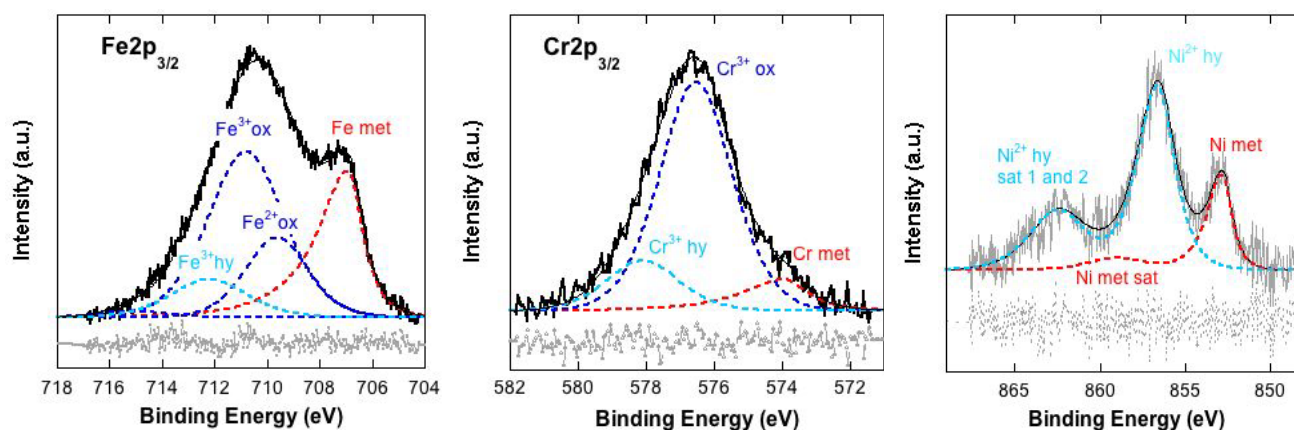


Figure 3: High-resolution XPS spectra of the surface film stainless grown on steels following the exposure to alkaline solution 0.1 M NaOH after background subtraction and curve fitting.

In this work only examples of the XPS spectra are presented (Fig. 3), the full details are provided in [9, 10]. The high-resolution spectra of all the elements show the presence of signals from the alloy beneath the passive film (e.g. Fe_{met}, Cr_{met}, Ni_{met}) and of signals from the metal ions in the

passive film, present in different oxidation state and as oxide and/or hydroxide. The binding energies for each component in the XPS spectra are in agreement with literature. For each element, the percentage of each component, due to different chemical states, is calculated from the area under the curve obtained in the curve fitting procedure.

The quantitative analysis was performed with the three-layer model [8] that allows to calculate the thickness and composition of the surface films based on the integrated intensities from curve fitting of the high-resolution spectra of a single XPS analysis. This quantitative calculation method provides average composition of the three layers (hydrocarbon layer due to contamination which occurs when the surface is exposed to the solution and to the environment, oxide-hydroxide passive film, metal beneath the passive layer). Actually, in depth composition gradients are present as shown with angle-resolved XPS for e.g. the manganese DIN 1.4456 steel [10].

Passive film composition. The results (Fig. 4) obtained on the alloys Fe15Cr, DIN 1.4301, DIN 1.4462 and the manganese bearing DIN 1.4456 stainless steels are similar for the two alkaline solutions and also for OCP exposure (Fig. 1) or potentiostatic passivation (Fig. 2). The content of iron oxide in the passive film progressively decreases with higher amount of alloying elements chromium, nickel / manganese and molybdenum. The chromium oxy-hydroxide content in the passive film increases from 45% for the Fe15Cr alloy and the stainless steel 1.4301 up to 55% for the 1.4462 duplex stainless steel. On the 1.4301 stainless steel surface films a marked enrichment of nickel in the passive film can be noted.

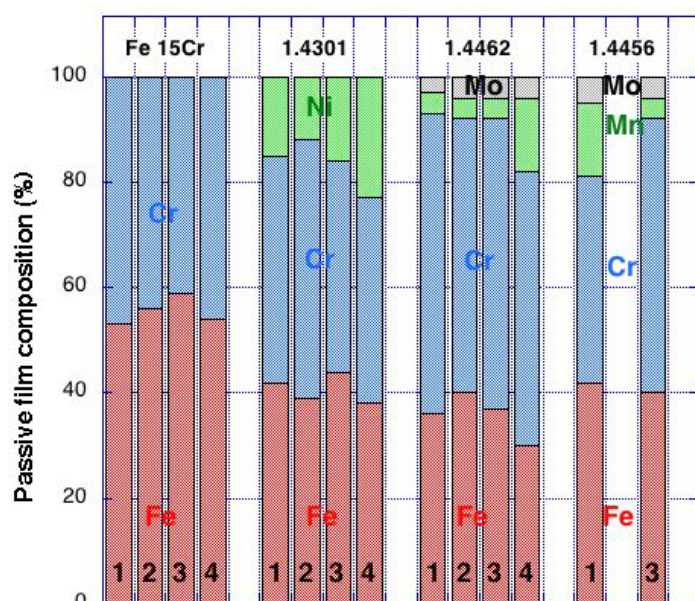


Figure 4: Composition of the passive films grown on the surface of mechanically polished stainless steels after 1 day exposure to alkaline solutions. For each material four different situations were analyzed:

- 1 0.1 M NaOH, OCP
- 2 0.1 M NaOH, passivated -0.1 V SCE
- 3 pore solution
- 4 pore solution, passivated -0.1 V SCE

The passive film of the nickel free DIN 1.4456 stainless steel showed the presence of about 6% oxidized molybdenum (Fig. 4). As molybdenum is well known to increase the resistance against pitting corrosion [11], the protective properties of the passive film against chloride-induced localized corrosion in alkaline solutions or concrete of the DIN 1.4456 stainless steel should be better than those of the DIN 1.4301.

Discussion

Stainless steels are used in all types of environments and also as reinforcement in concrete due to their high resistance against chloride-induced localized corrosion. In the following, two aspects will be discussed: first, the relation between the surface analytical results, especially the passive film composition, and the pitting potential in chloride bearing alkaline solutions, and second to the critical chloride content in concrete.

Relation to the pitting potential. The pitting potential E_{pit} is a measure for the resistance towards localized corrosion of the stainless steels in chloride bearing alkaline solutions. The pitting potentials E_{pit} obtained with potentiodynamic tests on black steel, low-alloyed chromium steels and stainless steels in saturated $\text{Ca}(\text{OH})_2$ solution with 5% chloride (ca. 1.5 M/dm^3) are reported in [12]. Black steel showed a pitting potential of -0.42 V SCE , the duplex stainless steel DIN 1.4462 did not show pitting and reached the oxygen evolution potential at $+0.6 \text{ V SCE}$. As shown in Fig. 5, E_{pit} increases linearly with the pitting resistance equivalent number (PREN) calculated as $\text{PREN} = \% \text{Cr} + 3.3\% \text{Mo}$ (Fig. 5, see also [9]). Included in Fig. 5 are also pitting potentials of three lean duplex steels determined in $\text{Ca}(\text{OH})_2$ solution with the same chloride concentration [13]. A similar relation between E_{pit} on the PREN was reported for higher alloyed stainless steels in 0.1 M NaOH solution with $1 - 5 \text{ M NaCl}$ added [9].

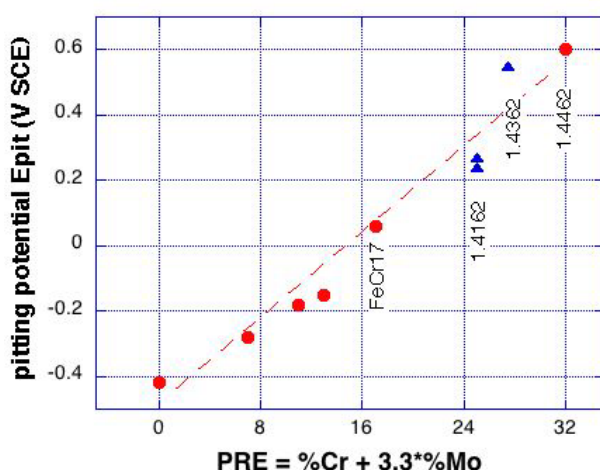


Figure 5: Pitting potentials of Fe-Cr alloys and stainless steels in sat. $\text{Ca}(\text{OH})_2$ solution with 5% chlorides [12, 13] plotted versus the PREN.

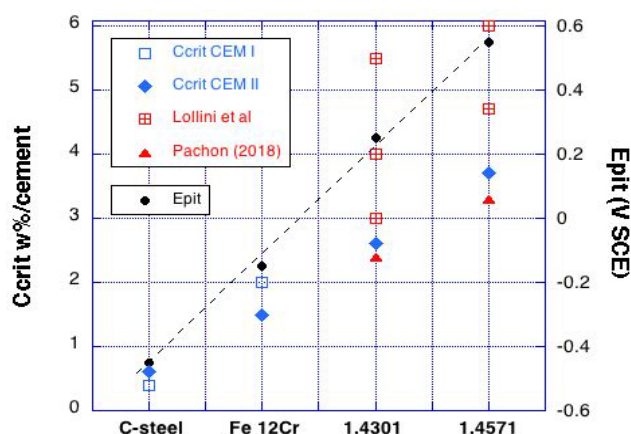


Figure 6: Critical chloride content C_{crit} for C-steel, Fe12Cr, 1.4301 and 1.4571 SS from literature [7, 14, 15].

Taking now into account the passive film composition (Fig. 4), it was proposed to calculate a value similar to PREN, but based on the percentages of the oxidized chromium and molybdenum present in the passive film, the so-called *composition index*. The value of the composition index was calculated as $\% \text{Cr}(\text{ox}) + 3.3\% \text{Mo}(\text{VI})\text{ox}$ and ranges from 45 for Fe15Cr alloy to 68 for 1.4462 stainless steel. The composition index based on XPS surface analytical results showed a linear relation to the pitting potential [9].

Relation to the critical chloride content C_{crit} in concrete. The experimental determination of the critical chloride content C_{crit} for the initiation of corrosion of steel in concrete is laborious and can take several months – for stainless steels with a much higher corrosion resistance even much longer. Thus a link to a more rapid test procedure, possibly experiments in solution, would be very helpful for engineers and owners that intend to use stainless steel reinforcement. Figure 6 shows, based on values for steels and stainless steels in concrete taken from literature [7, 14, 15], that C_{crit} shows the same increasing trend $\text{C-steel} < \text{Fe12Cr} < 1.4301 < 1.4571$ as the pitting potential determined in solutions [12, 13]. The pitting potential itself can be rationalized by the passive film composition [9], thus the relation C_{crit} for steels and stainless steels in concrete vs E_{pit} has a sound basis.

Despite this correlation, a quantitative prediction of the C_{crit} for different stainless steels in concrete has to take into consideration its inherent large variation (Fig. 6, [14, 15]). For new types of stainless steels with lower material costs such as lean duplex steels, at least a qualitative ranking of C_{crit} can be made based on the measured pitting potential in solution.

Conclusions

The knowledge of the critical chloride content C_{crit} of stainless steels in concrete is required to choose the most appropriate, corrosion resistant but not too expensive alloy. In this work own and literature data of pitting potentials of stainless steels in solution, XPS surface analysis of the passive film composition were confronted with C_{crit} . The following conclusions can be drawn:

- The critical chloride content C_{crit} for the corrosion onset of steel, Fe12Cr alloy, 1.4301 and 1.4571 stainless steels in concrete (determined with realistic, but time consuming tests) is related to the pitting potential obtained on alkaline solutions (short term test).
- An increasing chromium oxy-hydroxide content in the passive film determined by X-ray photoelectron spectroscopy increases the resistance to pitting corrosion and can explain the higher pitting potentials E_{pit} .
- Additional work is required to take into account the intrinsic stochastic variability of both C_{crit} and E_{pit}

References

- [1] L Bertolini, Steel Corrosion and service life of reinforced concrete structures, Structure and Infrastructure Management, Vol. 4 (2008) pp. 123 - 137,.
- [2] L. Bertolini, B. Elsener, P. Pedferri, E. Redaelli, R. Polder, Corrosion of Steel in Concrete – Prevention, Diagnosis, Repair, Wiley VCH 2nd edition, 2013.
- [3] Guidance on the use of stainless steel reinforcement, The Concrete Society, Technical Report No. 51, 1998.
- [4] C.M. Hansson, Corrosion of stainless steel in concrete, in Corrosion of Steel in Concrete Structures, ed. A. Poursaei. Woodhead Publishing, Elsevier, 2016.
- [5] P. Castro-Borges, O.T. de Rincón, E.I. Moreno, A.A. Torres-Acosta, M. Martínez-Madrid, A. Knudsen, Performance of a 60-year-old concrete pier with stainless steel reinforcement, Mater. Performance 41 (2002) 50-55
- [6] Markeset, G, Rostam, S. and Klinghoffer, O., Guide for the use of stainless steel reinforcement in concrete structure, Nordic Innovation Centre project-04118, Byggforsk report 405, ISBN 82-536-0926-4, 2006
- [7] F. Hunkeler, Use of stainless steel reinforcement in concrete structures, research report 543 (2000) Swiss Federal Department of the Environment, Transport, Energy and Communication (in German) download from mobilityplatform.ch
- [8] B. Elsener and A. Rossi, Passivation of Steel and Stainless Steel in Alkaline Media Simulating Concrete, Encyclopedia of Interfacial Chemistry, Elsevier (2018) pp. 365 - 375
- [9] B. Elsener, M. Fantauzzi, A. Rossi, Stainless steels: passive film composition, pitting potentials and critical chloride content, Materials and Corrosion, 71 (2020) 797 – 807
- [10] B. Elsener, S. Coray, D. Addari, A. Rossi, Nickel-free Manganese bearing stainless steel in alkaline media – electrochemistry and surface chemistry, Electrochimica Acta 56 (2011) 4489 – 4497
- [11] Ha, H.-Y.; Lee, T.-H.; Bae, J.-H.; Chun, D.W. Molybdenum Effects on Pitting Corrosion Resistance of FeCrMnMoNC Austenitic Stainless Steels. *Metals* 2018, 8, 653 - 666
- [12] U. Nürnberger, W. Beul, Corrosion of stainless steel reinforcement in cracked concrete, Otto Graf Journal 10 (1999) 23, https://www.mpa.uni-stuttgart.de/publikationen/otto_graf_journal/ogj_1999/beitrag_nuernberger.pdf

-
- [13] L. Bertolini and M. Gastaldi, Corrosion resistance of low-nickel duplex stainless steel rebars, *Materials and Corrosion* 62 (2011) 120 – 129
 - [14] F. Lollini, M. Carsana, M. Gastaldi, E. Redaelli, Corrosion behaviour of stainless steel reinforcement in concrete - Review, *Corros Rev* 37 (2019) 3 - 19
 - [15] A. Pachón-Montaña, J. Sánchez-Montero, C. Andrade, J. Fullea, E. Moreno, V. Matres, Threshold concentration of chlorides in concrete for stainless steel reinforcement: Classic austenitic and new duplex stainless steel, *Construction and Building Materials* 186 (2018) 495 - 502